

AFWAL-TR-84-3063

AD-8096070

STATIC AND FATIGUE BEHAVIOR OF PIN-LOADED
METAL MATRIX JOINTS

Frank M. Grimsley

Structural Integrity Branch
Structures and Dynamics Division

June 1984

Final Report for Period May 1983 - November 1983

Distribution limited to U.S. Government agencies only: test and evaluation; June 1984. Other requests for this document must be referred to AFWAL/FIBE, Wright-Patterson Air Force Base, Ohio 45433

SUBJECT TO EXPORT CONTROL LAWS

This document contains information for manufacturing or using munitions of war. Export of the information contained herein, or release to foreign nationals within the United States, without first obtaining an export license, is a violation of the International Traffic-in-Arms Regulations. Such violation is subject to a penalty of up to 2 years imprisonment and a fine of \$100,000 under 22 USC 2778.

Include this notice with any reproduced portion of this document.

FLIGHT DYNAMICS LABORATORY
AIR FORCE WRIGHT AERONAUTICAL LABORATORIES
AIR FORCE SYSTEMS COMMAND
WRIGHT-PATTERSON AIR FORCE BASE, OHIO 45433

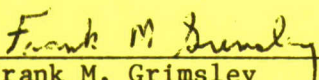


20071128137

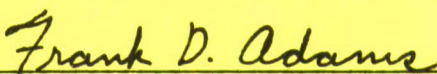
NOTICE

When Government drawings, specifications, or other data are used for any purpose other than in connection with a definitely related Government procurement operation, the United States Government thereby incurs no responsibility nor any obligation whatsoever; and the fact that the government may have formulated, furnished, or in any way supplied the said drawings, specifications, or other data, is not to be regarded by implication or otherwise as in any manner licensing the holder or any other person or corporation, or conveying any rights or permission to manufacture, use, or sell any patented invention that may in any way be related thereto.

This technical report has been reviewed and is approved for publication.

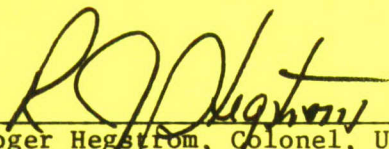


Frank M. Grimsley
Program Engineer
Structural Integrity Branch



Frank D. Adams, Chief
Structural Integrity Branch
Structures & Dynamics Division

FOR THE COMMANDER:



Roger Hegstrom, Colonel, USAF
Chief, Structures & Dynamics Division

"If your address has changed, if you wish to be removed from our mailing list, or if the addressee is no longer employed by your organization, please notify AFWAL/FIBE, W-PAFB, OH 45433 to help maintain a current mailing list."

Copies of this report should not be returned unless return is required by security considerations, contractual obligations, or notice on a specific document.

REPORT DOCUMENTATION PAGE

1a. REPORT SECURITY CLASSIFICATION UNCLASSIFIED		1b. RESTRICTIVE MARKINGS N/A	
2a. SECURITY CLASSIFICATION AUTHORITY N/A		3. DISTRIBUTION/AVAILABILITY OF REPORT Distribution limited to U.S. Government agencies only: test and evaluation; June 1983. Other request for this document must	
2b. DECLASSIFICATION/DOWNGRADING SCHEDULE N/A		4. PERFORMING ORGANIZATION REPORT NUMBER(S) AFWAL-TR-84-3063	
4. PERFORMING ORGANIZATION REPORT NUMBER(S) AFWAL-TR-84-3063		5. MONITORING ORGANIZATION REPORT NUMBER(S)	
6a. NAME OF PERFORMING ORGANIZATION Structural Integrity Branch Structures & Dynamics Division	6b. OFFICE SYMBOL (If applicable) AFWAL/FIBE	7a. NAME OF MONITORING ORGANIZATION	
6c. ADDRESS (City, State and ZIP Code) Wright-Patterson Air Force Base Dayton, OH 45433		7b. ADDRESS (City, State and ZIP Code)	
8a. NAME OF FUNDING/SPONSORING ORGANIZATION	8b. OFFICE SYMBOL (If applicable)	9. PROCUREMENT INSTRUMENT IDENTIFICATION NUMBER	
8c. ADDRESS (City, State and ZIP Code)		10. SOURCE OF FUNDING NOS.	
		PROGRAM ELEMENT NO.	PROJECT NO.
		TASK NO.	WORK UNIT NO.
11. TITLE (Include Security Classification) Static and Fatigue Behavior of Metal Matrix Joints (U)		62201F	2401
		01	79
12. PERSONAL AUTHOR(S) GRIMSLEY, FRANK M.			
13a. TYPE OF REPORT Final	13b. TIME COVERED FROM <u>May 83</u> TO <u>Nov 83</u>	14. DATE OF REPORT (Yr., Mo., Day) June 1984	15. PAGE COUNT 37
16. SUPPLEMENTARY NOTATION			
17. COSATI CODES		18. SUBJECT TERMS (Continue on reverse if necessary and identify by block number)	
FIELD	GROUP	SUB. GR.	
11	04		Metal Matrix Composites Silicon Carbide/Aluminum Continuous-Fiber-Reinforced Aluminum B ₄ C/Aluminum
19. ABSTRACT (Continue on reverse if necessary and identify by block number) Unidirectional Metal Matrix Composite Pin-loaded joints were experimentally evaluated. Conventional composite joint analysis was used to predict the failure loads. Good agreement was obtained between experiment and analysis.			
20. DISTRIBUTION/AVAILABILITY OF ABSTRACT UNCLASSIFIED/UNLIMITED <input type="checkbox"/> SAME AS RPT. <input checked="" type="checkbox"/> DTIC USERS <input type="checkbox"/>		21. ABSTRACT SECURITY CLASSIFICATION UNCLASSIFIED	
22a. NAME OF RESPONSIBLE INDIVIDUAL FRANK M. GRIMSLEY		22b. TELEPHONE NUMBER (Include Area Code) (513)255-6104	22c. OFFICE SYMBOL AFWAL/FIBE

3. be referred to AFWAL/FIBE, Wright-Patterson Air Force Base, Ohio 45433

- 18. Boron/Aluminum
- Unidirectional Composites
- Hybrid Composites
- Titanium Cladding
- Pin-loaded joints
- joints
- mechanically fastened joints
- joint analysis
- fatigue
- mechanical testing

Foreword

This report describes an in-house effort conducted under Project 2401, "Structures and Dynamics," Task 240101, "Structural Integrity for Military Aerospace Vehicles," Work Unit 24010109, "Life Analysis and Design Methods for Aerospace Structures."

The work was performed by the Structural Integrity Branch, Structures and Dynamics Division, Flight Dynamics Laboratory, Air Force Wright Aeronautical Laboratories (AFWAL/FIBE), Wright-Patterson Air Force Base, Ohio. The research was conducted under the direction of Frank M. Grimsley from May through November 1983.

The author wishes to acknowledge the support of Mr. Charles Saff of the McDonnell Douglas Aircraft Company for supplying some of the material used in this program and the helpful technical advice. The author also wishes to thank Dr. George Sendekyj for his technical consultations and advice. In addition the author wishes to thank H. Stalnaker, R. Kleismit and J. Smith for their assistance with the structural testing, P. Rimer and D. Oliviera, both of Beta Industries, Inc., for their help with specimen fabrication and specimen dissections, Messrs. R. Henderson and J. Ziegenhagen of AFWAL/MLSA for the electron microscopy, N. Tracy of Universal Technology, Inc. for the nondestructive testing and finally L. Bates for the optical microscopy and photography.

The completed report was submitted in December 1983.

TABLE OF CONTENTS

SECTION	PAGE
I INTRODUCTION	1
II EXPERIMENTAL PROCEDURE	2
1. Materials	2
2. Specimen Fabrication Procedures	3
3. Mechanical Testing Procedures	3
III MECHANICAL PROPERTY TEST RESULTS AND ANALYSIS	5
1. Mechanical Property Test Results	5
2. Rule of Mixtures Analysis of the Longitudinal Stress-Strain Behavior	6
3. Experimental Determination of Broken Fibers in SiC/Al	9
4. Prediction of the Longitudinal Modulus vs. Strain Curves	10
5. Transverse Stress-Strain Results	12
IV PIN-BEARING JOINT TEST RESULTS	13
1. Experimental Results	13
2. Analytical Procedures	14
3. Analytical Results	16
4. Titanium Clad B ₄ C/Al Joint Results	16
V FATIGUE TEST RESULTS OF THE PIN-BEARING JOINTS	18
1. Analysis	18
2. Experimental Results	19
VI SUMMARY	20
VII CONCLUSIONS	22
VIII REFERENCES	23

LIST OF ILLUSTRATIONS

FIGURE		PAGE
1	Pin-Bearing Joint Specimen	25
2	Tensile Test Specimen	25
3	Pin-Bearing Test Assemblage	26
4	Full Range Stress-Strain Curves	27
5	SiC/Al Composite and Matrix Stress-Strain Curves	28
6	Scanning Electron Microscope Photographs Of "Limp" Fibers	29
7	Rule of Mixtures Predictions of Elastic Modulus vs. Strain	30
8	Scanning Electron Microscope Photographs of the Failure Surface of a B_4C/Al Composite clad with Ti-6Al-4V	31
9	Typical Static Pin-Bearing Joint Failures	32

LIST OF TABLES

TABLE		PAGE
1	Measured Material Property Data	33
2	Experimental vs. Analytical SiC/Al Specimen Dissection Results	33
3	Fiber and Matrix Properties used in Rule of Mixtures Analysis	34
4	Rule of Mixtures vs. Literature Fiber Moduli	34
5	Experimental Ultimate Failure Loads and Modes for the Static Pin-Bearing Specimens	35
6	Average Bearing Stresses for the Pin-Bearing Specimens	35
7	Mechanical Properties used in BJSFM Analysis	36
8	BJSFM Predictions vs. Experimental Results	36
9	Fatigue Test Results	37

SECTION I

INTRODUCTION

Continuously reinforced metal matrix composites (MMC) have been projected to have the potential to save weight in aerospace structures due to their high strength and stiffness.¹⁻⁴ These structures must somehow be joined together to form larger structures. Historically, the most common and most accepted method of joining structures together is through the use of fasteners with varying amounts of load transfer between them. These types of loadings are very complex and are not well understood even in conventional metals. Some work has been done for the graphite/epoxy composites but very little has been done on continuously reinforced MMC. In the early 1970's, design allowables were attempted for continuous Boron fiber reinforced Aluminum (B/Al)⁵. This work included some experimental single-lapped shear joint data. The object of the effort was to develop statistically significant data for use in detail design. No attempt was made to understand its behavior from a microscopic viewpoint nor was an attempt made to predict the failure loads. No data was generated on the fatigue behavior of the joints.

The objective of the current study was to assess the ability of current composite analysis procedures to predict the static behavior of joints made from various unidirectional MMC and to investigate the fatigue behavior of these joints when subjected to constant amplitude loading. Specific objectives were to determine experimentally the static behavior of double-lapped shear joint specimens made from three different MMC composites; to analytically predict the static strength of these joints and to experimentally determine whether joints under fatigue loading fail in the same manner as the statically loaded joints.

SECTION II

EXPERIMENTAL PROCEDURE

1. MATERIALS

Three different materials were tested. The three materials are (1) unidirectional, 8-ply boron-fiber-reinforced 6061 aluminum (B/Al), (2) unidirectional silicon-carbide-fiber-reinforced 6061 aluminum (SiC/Al) and (3) unidirectional, 2-ply borsic-fiber-reinforced 6061 aluminum (B_4C/Al) clad with 0.005-inch-thick Ti-3Al-2.5V.

The SiC/Al was manufactured in 1980 by AVCO. It was manufactured by a plasma spray concept. In this concept, a preform is made by collomating the fibers and then spraying them in place with an atomized plasma-spray of aluminum. The preforms are then layed up and hot-molded using a pressure/vacuum bag method similar to that used in conventional graphite/epoxy composites. The properties of this SiC/Al should not be considered typical of present-day SiC/Al because at that time the fiber manufacturing process was still being developed. The SiC/Al was tested in this program because it was felt that it would represent the low end of properties and behavior and would therefore provide information on how susceptible this class of material is to microstructural differences.

The B/Al was manufactured in 1983 by Amercom, Inc.. The material was manufactured by a vacuum diffusion bonding process by means of a hot press. This material represents the state-of-the-art in MMC materials. It's mechanical properties have been well-characterized.

The B_4C/Al , clad with Ti-3Al-2.5V titanium, was manufactured in 1979 by Amercom in similar fashion to that of the B/Al. The titanium cladding was used to increase it's transverse strength. This material was chosen for this program for two reasons. First, to determine if the cladding would increase the joint strength and ,secondly, to examine the capability of analytical methods to analyze hybrid composites.

A detailed study of the failure mechanisms of these materials was performed using radioactive-dye-enhanced radiography and scanning electron microscopy (SEM). Some specimens were destructively examined by etching away the matrix, using Sodium Hydroxide, and then examining the amount of broken fibers found within the specimen.

2. SPECIMEN FABRICATION PROCEDURES

All specimens were cut from flat panels with a diamond saw and their edges sanded with diamond paste. Tapered diamond-coated carbide drill bits were used to drill all the holes. Each panel and one specimen of each geometry were radiographed to determine the initial quality of the panels and the effect of machining on the specimens. No evidence of damage was noted on either the panels or the specimens.

3. MECHANICAL TESTING PROCEDURE

All tensile tests were performed on a mechanical "screw type" Instron testing machine at a displacement rate of 0.2 inch/minute. Load resolution on this machine is 1.5% over its entire load range. Back-to-back strain gages were used on all material property test specimens to generate full-range stress-strain curves in both the longitudinal and transverse directions for each material. Some specimens were instrumented with back-to-back rosette strain gages to measure Poisson's ratio. The material property test and the pin-bearing joint specimens were 0.5 and 1.5 inches wide respectively. All specimens were 7 inches long. Fiberglass tabs were bonded onto the ends of the specimens to prevent the loading grips from crushing the fibers. Specimen details are shown in figures 1* and 2. The fatigue specimen's geometry was the same as the tensile joints.

* Figures and tables are located at the end of the report

The pin-bearing tests were performed by inserting the specimen between two flat sheets of aluminum. Shims were inserted between the sheets of aluminum to support the ends opposite the specimen. The complete assemblage was then placed in the loading machine. Assemblage details are shown in figure 3.

Load-displacement curves were generated for the pin-bearing joint (PBJ) specimens using a strip chart recorder. The maximum load on the load-displacement curve was considered the failure load for the pin-bearing specimens. Triplicate specimens were used in all the tests.

All fatigue tests were performed on a servo-hydraulic axial loading frame. The load resolution on this machine is 1.0% over its entire load range. All loading was constant amplitude at a minimum to maximum stress ratio (R) of 0.1 at an applied cyclic frequency of 30 Hz. The loads were determined by analytical calculations detailed in the analysis segment of Section V. Failure was assumed to occur when the joint displaced 0.05 in. as measured by displacement gages inside the test machine.

SECTION III

MATERIAL PROPERTY TEST RESULTS AND ANALYSIS

1. MECHANICAL PROPERTY TEST RESULTS

The ultimate strength, Poisson's ratio, Young's tensile modulus and strain-to-failure for both the longitudinal and transverse directions were determined for each material. Table 1 contains the material property data generated in this program. Since all of these materials exhibit nonlinear behavior, especially in the transverse direction as shown in figure 4, the modulus values listed in table 1 are valid for low strain levels only.

The SiC/Al and the B/Al had different longitudinal stress-strain curves as shown in figure 4. As can be seen from figure 4, the SiC/Al stress-strain curve is nonlinear. Theoretically, the SiC/Al and the B/Al should have similar material behavior because the fibers used in both of them have similar material properties and 6061 aluminum was used in both as the matrix material. Therefore, the nonlinear stress-strain curve of the SiC/Al will be further investigated.

In figure 5, an excellent agreement between the strain value at onset of nonlinear behavior of the SiC/Al and the strain value at onset of yielding in 6061 aluminum is shown. Therefore, the nonlinearity of the SiC/Al stress-strain curve is related to the nonlinearity of the matrix stress-strain curve. This relationship is precisely what Spencer⁶ postulated for a composite with elastic fibers and an elastic, perfectly plastic matrix. This theory is commonly referred to as the rule of mixtures. Therefore a simple rule of mixtures analysis can be used to analyze the nonlinear longitudinal behavior of the SiC/Al.

The stress-strain curve of the SiC/Al can be broken into three distinct regions as shown in figure 5. Region I of the SiC/Al stress-strain curve is the strain range in which the Young's modulus of both the fiber and the matrix are linear. Region II of the stress-strain curve is the strain range where the Young's modulus of the matrix varies with strain level and the Young's modulus of the fibers remain constant. Finally, in region III, the Young's modulus of the matrix is zero and the fiber modulus is constant. This type of matrix behavior assumes the matrix eventually becomes perfectly plastic.

2. RULE OF MIXTURES ANALYSIS OF THE LONGITUDINAL STRESS-STRAIN BEHAVIOR OF SIC/AL

The rule of mixtures for longitudinal modulus is

$$E_c = E_f v_f + E_m (1 - v_f) \quad (1)$$

where:

E_c = composite modulus

E_f = fiber modulus

E_m = matrix modulus

v_f = fiber volume fraction

As can be seen from eq. 1, three factors greatly affect its longitudinal modulus. One of these, the Young's modulus of the ceramic silicon carbide fiber is constant to failure. Therefore, only v_f and E_m can cause the SiC/Al modulus to decrease with increasing strain level.

The maximum contribution of the matrix to the overall composite modulus can be determined by outermost right hand term of eq. 1. The volume fraction of the SiC/Al as supplied by the manufacturer was 0.48 and the initial secant modulus of 6061-T4 aluminum is 9.9 Msi. Substituting these values into eq. 1 and letting the fiber modulus be zero yields 5.2 Msi. This is the maximum contribution that the matrix can have to the composite's overall longitudinal modulus.

The minimum value of modulus the matrix can have is zero assuming the matrix becomes perfectly plastic. Therefore based on eq. 1, as the composite is strained its modulus should decrease by no more than 5.2 Msi. The initial modulus of the composite was 31.5 Msi. Therefore, the final modulus should be $31.5 - 5.2$ or 26.3 Msi. The experimental value of the final modulus was 23.0 Msi. This is below the minimum value of final modulus assuming the matrix is entirely responsible for the nonlinear behavior. Therefore, it can be concluded that the matrix is not entirely responsible for the nonlinear behavior of the composite.

The only term other than the matrix modulus that can vary with strain level is the fiber volume fraction. This implies that fibers are breaking in the composite as it strains. Solving eq. 1 for v_f and assuming that at failure the matrix is perfectly plastic, the final fiber volume fraction can be estimated. The final fiber volume fraction, v_f^f , can be computed based on the above assumption from the reduced equation (1).

$$v_f^f = E_c/E_f \quad (2)$$

Using a modulus of 60 Msi for the modulus of silicon carbide fiber, eq. 2 yields 0.38 as the final volume fraction.

The actual number of broken fibers the final volume fraction represents can be approximated by the following equation.

$$N_f = (4v_f Wt) / (\pi D^2) \quad (3)$$

where:

W = width of the specimen

D = diameter of the fiber

N_f = number of broken fibers in
the specimen

t = thickness of the specimen

The silicon fibers are nominally 0.0056 inch in diameter and the width of the tensile specimens was 0.5 inch. Substituting these values into eq. 3 and using the initial fiber volume fraction, 0.48, the number of fibers in the specimen was found to be 492. The number of fibers in the specimen after straining it into region III was 394, using the final fiber volume fraction, 0.38, in place of the initial fiber volume fraction in eq. 3.

The difference between the initial number of fibers in the specimen and the number of fibers in the specimen after straining it into region III is the number of fibers broken in a specimen going from initially unstrained into region III of figure 5. Therefore, eq. 3 predicts 98 fibers were broken during straining.

3. EXPERIMENTAL DETERMINATION OF BROKEN FIBERS IN SiC/Al

To verify the results predicted previously, several specimens were strained into region II and III, respectively, of figure 5 and then unloaded. These specimens, together with a specimen that had not been strained, were destructively examined by etching away the matrix with a Sodium Hydroxide (NaOH) solution. Silicon Carbide is inert to NaOH and is not harmed by the etching process.

The destructive evaluation found a few fiber breaks as shown in table 2. These broken fibers constitute less than 5% of the total number of fibers in the specimens and are therefore considered not significant. Also, the number of broken fibers in the specimen loaded into region II was equivalent to the number in the specimen loaded into region III. Therefore, most of the fibers that broke, failed before they were strained into region III.

A significant finding, however, was the presence of a large percentage (~ 15%) of the fibers that seemed to have very little stiffness and appeared unbroken. A careful examination of these "limp" fibers using SEM revealed that in these "limp" fibers the SiC had broken away from the tungsten core. Figure 6 shows typical SEM photographs of the fibers. Photograph A of figure 6 shows longitudinal cracks as well as the Silicon Carbide broken away from the Tungsten core. Photograph B shows transverse cracks in the fiber. Both of these fibers were taken from the specimen which was not loaded and are typical of the fibers found in both the loaded and unloaded specimens.

Since the SiC is partially broken away from the tungsten core, the total load in the fiber must be carried by the tungsten core in the areas where the SiC is broken away. This would cause the stress in the tungsten wire to be very high in those locations. The tungsten wire does not break during loading because its strain-to-failure (>10%) is much higher than the strain-to-failure of the SiC/Al composite.⁷⁻⁸ It does, however, go plastic and yield, which causes its tangent modulus to be much less than its elastic modulus of 50 Msi. Therefore the tungsten wire contributes little to the overall tangent modulus of

the composite. These "limp" fibers can be assumed to behave like broken fibers which also contribute nothing to the overall tangent modulus of the composite. The number of broken fibers predicted, previously, is in excellent agreement with the experimentally determined number of "limp" and broken fibers found in the specimens.

Because of the large percentage of "limp" fibers found in the specimens, the fiber volume fraction of the composite is effectively reduced. This reduced fiber volume fraction is given by

$$v_f^e = [(\pi/4)D^2/(Wt)](N_f - N_{dam}) \quad (4)$$

v_f^e = effective fiber volume fraction
 N_{dam} = number of broken or limp
 fibers initially in the
 composite

Equation 4 yields an effective fiber volume fraction of 0.39 for an average N_{dam} of 88 "limp" fibers for the three specimens.

4. PREDICTION OF THE LONGITUDINAL MODULUS VS. STRAIN CURVES

The rule of mixtures, eq. 1, can now be used to predict the longitudinal stress strain behavior of SiC/Al and the B/Al. Eq. 1 can also be used to predict the stress-strain behavior of the hybrid Titanium clad B₄C/Al by expanding the matrix term to include the titanium.

$$E_c = E_f v_f + E_{al} v_{al} + E_{ti} v_{ti} \quad (5)$$

The stress-strain behavior of these materials can now be predicted by substituting the tangent moduli of both 6061-T4 and Ti-3Al-2.5V. The tangent moduli for 6061-T4 was taken from figure 5. The titanium does not yield for the strain-to-failures in these composites and therefore a value of 14.4 Msi was used for all strain levels in these analyses.²

In section 3, an assumed longitudinal Young's modulus for the fiber was used to estimate the fiber volume fraction based on the number of broken fibers in the specimens. This estimated fiber volume fraction was then compared to the experimentally determined fiber volume fraction. In this section, the experimentally determined fiber volume fraction for SiC/Al and reported volume fractions for the other materials will be used to estimate the fiber's longitudinal Young's moduli.

The properties of the components used in these analyses are listed in table 3. The fiber modulus values were obtained by substituting the composite modulus obtained from table 1 into eq. 1 and solving for the fiber modulus as shown.

$$E_f = [E_c - E_{al}v_{al} - E_{Ti}v_{Ti}]/v_f \quad (6)$$

The results of eq. 6 agree very well with the reported fiber moduli as shown in table 4.

Using the values from table 3, the tangent stress-strain curves of all three metal matrix composites were calculated using eqns 1 and 5. Figure 7 shows the results of the analysis. As can be seen from the figure, Rule of Mixtures predicts their longitudinal behavior very well.

5. TRANSVERSE STRESS-STRAIN RESULTS

The transverse stress-strain behavior of these composites is a matrix-dominated property. The failure load of the B/Al is essentially the failure load of the matrix. The transverse modulus of the composite was almost twice that of the matrix material due to the presence of the fibers. The failure strains were lower than the corresponding failure strains of the matrix. This is due to the low strain-to-failure of the fiber-matrix interface. The SiC/Al had the identical transverse modulus of the B/Al, however its strain-to-failure was lower resulting in a lower transverse strength than the B/Al due to the very low strain-to-failure of its matrix-fiber interface. If this matrix-fiber interface could be strengthened, the SiC/Al should behave identically to the B/Al.

In the titanium-hybrid-composite, the transverse modulus of the composite was very close to that of B/Al and SiC/Al. However, its strain-to-failure is higher than either B/Al or SiC/Al. Figure 8 shows SEM photographs of the titanium-composite interface showing a separation between the titanium foil and the aluminum matrix. It appears that, as the composite strains, the titanium-composite interface begins to fail locally.

SECTION IV

STATIC PIN-BEARING JOINT TESTS

1. EXPERIMENTAL RESULTS

The ultimate failure loads of the pin-bearing joint (PBJ) specimens were determined for each metal matrix composite specimen. The failure loads and failure modes are presented in Table 5. The ultimate bearing strength and net tension stresses are shown in table 6.

As can be seen from Table 6, the lowest bearing stress was obtained for the SiC/Al. The Ti-clad hybrid B_4C/Al and the B/Al had the same bearing stress as that of 6061 aluminum which is 90 Ksi. Therefore the bearing stress of these two materials is strongly related to the bearing stress of the matrix material. The low bearing stress of the SiC/Al is probably related to its low transverse strength and strain-to-failure which would cause premature bearing failure.

Photographs of typical failures for each material are shown in figure 9. Figure 9a. shows a typical B/Al joint failure which borders on a shear-out failure. Other B/Al specimens were loaded to higher strains and the failure remained predominately bearing. In the SiC/Al (fig. 9b.), note the large longitudinal crack which forms from the edge of the specimens and progresses toward the hole. This is typical of the SiC/Al pin-bearing joint specimens. The titanium clad B_4C/Al (fig. 9c.) bearing failure was very similar in appearance to bearing failures in isotropic metals.

2. ANALYTICAL PROCEDURES

The analytical results were obtained from a computer program called "Bolted Joint Stress Field Model (BJSFM)".⁹ Briefly, the program performs a static strength analysis of isotropic and anisotropic materials at an individual fastener hole, both loaded and unloaded. The program also has the capability to handle hybrid-composite laminates. The program uses a closed form analytical approach based on elastic anisotropic theory of elasticity and laminated plate theory.

Table 7 shows all the mechanical properties used in the analysis. Data from the literature were used to obtain material properties not experimentally measured on these specific materials. In the case of the Ti clad B₄C/Al, some of the properties of the B₄C/Al were determined by elastic laminated plate theory. Also, the mechanical properties for the titanium are for Ti-6Al-4V, because the mechanical property data base for Ti-3Al-2.5V is not complete. The major difference between Ti-6Al-4V and Ti-3Al-2.5V is that the latter has approximately a 70% lower ultimate strength value. This difference would not be expected to change the analytical predictions a great deal.

In failure analysis of composites, the failure stresses must be calculated at a finite distance from the hole. This distance is sometimes referred to as the characteristic crack length and varies with material system and layup. Waddoups¹⁰ et al postulated that this characteristic crack length for predicting the fracture toughness of graphite/epoxy could be written as

$$K_c = S_c \sqrt{\pi(a+r)} \quad (8)$$

where:

K_c = fracture toughness

S_c = ultimate failure stress of notched laminate

r = characteristic crack length

a = notch length

This expression is very similar to a plastic zone correction factor used for predicting fracture in metals.

Awerbuch¹¹ experimentally determined r for B/Al laminates with holes by letting the crack length equal zero. The B/Al in this program had very similar properties to that of the type II B/Al listed in table II of reference 11. Note that a typographical error exists in the table and the value for r should be 0.07 inch. Since no data was found in the literature for the SiC/Al or the Ti clad B₄C/Al, an r value of 0.07 inch was assumed. This value of r was used for all the analytical predictions using BJSFM.

Dvorak¹² and others have shown that the matrix in these composites yields in shear at very low strain levels. Therefore plasticity effects must be included in their analysis. Since, BJSFM is a linear elastic model and uses linear composite theory to calculate the stresses, it does not take into account the nonlinearity of the MMC specimens and would predict very early shear failures in the composite. To predict the failure of the joints, the low failure load predicted by BJSFM is ignored, and the program is allowed to find the next failure mode by reducing the shear modulus of the composite to 1 Ksi. This is equivalent to allowing the matrix to yield in shear (assuming elastic-perfectly plastic matrix behavior).

This points out that BJSFM or any other purely elastic prediction technique must be used with caution when the strain levels in the metal matrix composite are such that the mechanical properties of the composite become nonlinear.

3. ANALYTICAL RESULTS

Using BJSFM and the material properties in Table 7, analytical predictions were made for the pin-bearing specimens. The Tsai-Hill failure criteria was used to determine failure of the laminate. The results of the analysis are shown in Table 8. As can be seen the analytical results agree within 10% of the experimental value.

4. Ti-Clad B₄C/Al Joint Results

The hybrid Ti-clad B₄C/Al did not exhibit an ultimate bearing stress significantly greater than the unidirectional B/Al, even though its transverse strength and strain-to-failure were much greater. This is because of the longitudinal Young's modulus mismatch between the B₄C/Al and the Titanium. The B₄C/Al has a longitudinal Young's modulus twice that of the titanium, resulting in the B₄C/Al loading up faster than the titanium.

BJSFM predicts the titanium was stressed only 75% of the B_4C/Al when the B_4C/Al fails. The load carried by the hybrid composite is immediately transferred to the titanium which increases the stress in the titanium significantly owing to the reduction in area. The stress in the titanium is now very close to that of its ultimate bearing strength and fails with very little increase in load. The titanium, therefore, contributes very little to the overall bearing stress of the hybrid.

SECTION V

FATIGUE TEST RESULTS OF PIN-BEARING JOINTS

1. ANALYSIS

Shakedown is the ability of a material to resume elastic deformation behavior after a number of plastic strain cycles. Simply put, if the stress level in a given material is below its shakedown limit stress, the material would not be expected to fail in fatigue; conversely, if its stress level is above its shakedown limit stress, the possibility exists that the material will begin to incur fatigue damage. Dvorak and Tarn¹² have experimentally determined that such a relationship exists between fatigue and shakedown in metal matrix composites.

Dvorak and Johnson¹³ experimentally determined the shakedown limit stress for unidirectional B/Al. It is given by the following equation.

$$S_{sh} = 6.1 Y / (1-R) \quad (9)$$

Y = yield stress of the matrix

R = stress ratio (min. stress/max. stress)

S_{sh} = shakedown limit stress

The onset of yielding in 6061-T0 aluminum occurs at a stress level of 8.4 Ksi according to Dvorak and Johnson. The stress ratio of the fatigue tests in this program is 0.1. Therefore, eq. 9 predicts the shakedown stress of the composite to be 57 Ksi.

All of the fatigue specimens, except one, were tested at fifty percent of their respective static bearing failure load. According to BJSFM, this results in a local stress at the edge of the hole of 66 Ksi, which is above the shakedown stress and they would be expected to fail in fatigue. One B/Al joint specimen was run at 23% of it's ultimate bearing stress, which results in a local stress at the edge of the hole of 30 Ksi. This stress is well below the shakedown limit stress, and the specimen should not fail in fatigue.

2. EXPERIMENTAL RESULTS

As expected, the specimens run above the shakedown stress level failed in fatigue. The test results are shown in Table 9. Note that the SiC/Al had more than a factor of 3 longer life than the B/Al specimens, even though it had the lowest ultimate bearing stress. Also note that the titanium-clad B₄C/Al had a factor of 3 shorter life than the B/Al specimens. The failure modes of all the joints were identical to that of the unfatigued static joints.

The B/Al joint, loaded cyclicly at 23% of its static failure load, did not fail in fatigue after 5 million cycles. These data, along with the other fatigue tests, seem to support the shakedown model developed by Dvorak and Johnson. The specimen was statically tested to failure to determine it's residual strength. It failed in bearing at 86.6 Ksi which is within the data scatter of the static joint bearing strengths.

SECTION VI

SUMMARY

This study was undertaken to assess the ability of current composite technology to predict the static behavior of double-lapped joints made from various unidirectional MMC materials and to investigate the fatigue behavior of these joints when subjected to constant amplitude loading. Three composite materials were chosen for testing. They were unidirectional B/Al and SiC/Al as well as a Ti clad unidirectional B_4C/Al hybrid. Detailed studies of the materials' behavior were made for both the static and fatigue tests using both destructive and nondestructive evaluation methods.

All of the joints for all three materials failed in pure bearing at loads nearly equivalent to the ultimate bearing stress of 6061-T4 aluminum. The matrix material is 6061-T4, but the actual heat treat of the matrix is not known after the aluminum goes through the temperature cycle used to consolidate the composite. In any event, due to the similarity of the failure mode and ultimate stress between the composite and pure aluminum it appears that the failure stress of the composite is strongly related to the failure stress of the matrix.

The hybrid composite, as expected, had a much higher transverse strength than the other composites. This did not increase its bearing strength, however. This was due to the elastic modulus difference between titanium and B_4C/Al which caused the B_4C/Al to load up faster than the titanium. Therefore, when the B_4C/Al failed the titanium took all the load and failed immediately because of its reduced area. The titanium, while increasing the transverse strength, did not contribute any bearing strength to the hybrid composite.

BJSFM, an elastic composite joint stress program was successfully used to predict the static failure loads of joints made from metal-matrix-composite materials. It had the ability to predict even complex hybrid materials to within 10%. Some limitations should be noted, however. In all cases, BJSFM predicted low shear stress failures that in reality had not occurred. The reason for which is the low shear yield stress of these materials, which BJSFM cannot account for. The low shear failures were disregarded by lowering the shear modulus of the composite. BJSFM was then used to calculate a failure load based on that assumption..

In order to use BJSFM, a characteristic distance from the free edge must be supplied that locates the point at which the failure stresses are to be calculated. It has been shown that relatively simple notched fracture test data can be used to experimentally determine that distance.

Dvorak and Johnson have developed a shakedown model that had previously been used on unloaded hole and simple tension specimens subjected to constant amplitude fatigue loading. This analysis along with a stress analysis of the joint from BJSFM was used successfully to predict whether the joints would fail in fatigue or not. One joint specimen, which was predicted not to fail in fatigue, did not fail after five million constant amplitude fatigue cycles. The joint was then statically loaded to failure. The failure load was on the low end but still within the data scatter of the unfatigued specimens. This result is consistent with the experimental work done by Dvorak and Johnson.

SECTION VII

CONCLUSIONS

1. It appears from these limited tests that the ultimate bearing strength of the composite is dependent on the bearing strength of the matrix. Therefore, if the bearing strength of the matrix were increased the ultimate bearing strength of the composites would also increase.

2. For this study, it appears that the titanium-clad B_4C/Al hybrid has no ultimate bearing strength advantage over an unclad MMC composite.

3. BJSFM proved to be an accurate tool for analyzing the bolted joints tested in this program. Caution should be exercised when applying this linear elastic stress model to nonlinear metal matrix materials when strain levels are such that extensive yielding of the matrix is occurring.

4. In fatigue, the MMC joints failed in pure bearing, the same manner as the static joints.

5. While there was a limited amount of data on fatigue of MMC joints developed in this program, the results are encouraging that the shakedown model does hold promise for analyzing MMC joints in a fatigue environment. More work must be done, however, to establish the bounds of the shakedown limit stress and how that stress is affected by load history and material variability.

SECTION VIII

REFERENCES

1. B.T. Gannon, D.E. Sherrill, P.J. Blaser, "Metal Matrix Composites Applications/Payoff for High Performance Aircraft Airframes," AFWAL-TR-81-3018, November 1980.
2. G.J. Inuaki, "Application of Metal Matrix Composite Materials to Missile Airframes," AFWAL-TR-3140, December 1980.
3. "Applications of Reinforced Metals to Cargo/Bomber Aircraft," AFWAL-TR-3061, June 1981.
4. A.V. Hawley, "Applications of Reinforced Metals to Cargo/Bomber Aircraft," AFWAL-TR-80-3147, February 1981.
5. R. Cairo and R. Torczyner, "Graphite/Epoxy, Boron-Graphite/Epoxy Hybrid and Boron/Aluminum Design Allowables," AFML-TR-72-232, March 1973.
6. A.J.M. Spencer, Deformations of Fibre-Reinforced Materials, Oxford, Clarendon Press, 1972.
7. Metals Handbook, vol. I, 8th Ed., "Properties and Selection of Metals," ASM.
8. Rare Metals Handbook, 2nd. ed., Clifford A. Hampel, ed., Reynolds Publishing Corp., Chapman & Hall Ltd., London, 1961.
9. J.M. Ogonowski, "Effect of Variances and Manufacturing Tolerances on the Design Strength and Life of Mechanically Fastened Composite Joints," Vol. 3, Bolted Joint Stress Field Model (BSJFM) Computer Program User's Manual, AFWAL-TR-81-3041, April 1981.

10. M.E. Waddoups, J.R. Eisenmann, and B.E. Kaminski, "Macroscopic Fracture Mechanics of Advanced Composite Materials," Journal of Composite Materials, Vol. 5 (October 1971), pp. 446-454.
11. J. Awerbuch and H.T. Hahn, "Crack-Tip Damage and Fracture Toughness of Boron/Aluminum Composites," Journal of Composite Materials, Vol. 13 (April 1979), pp. 82-107.
12. G. Dvorak and J. Tarn, "Fatigue and Shakedown in Metal Matrix Composites," ASTM-STP 569, Fatigue of Composite Materials, Society of Testing and Materials, 1975.
13. G. Dvorak and W.S. Johnson, "Fatigue of Metal Matrix Composites," International Journal of Fracture, Vol. 16, No. 6 (December 1980), pp. 585-607.

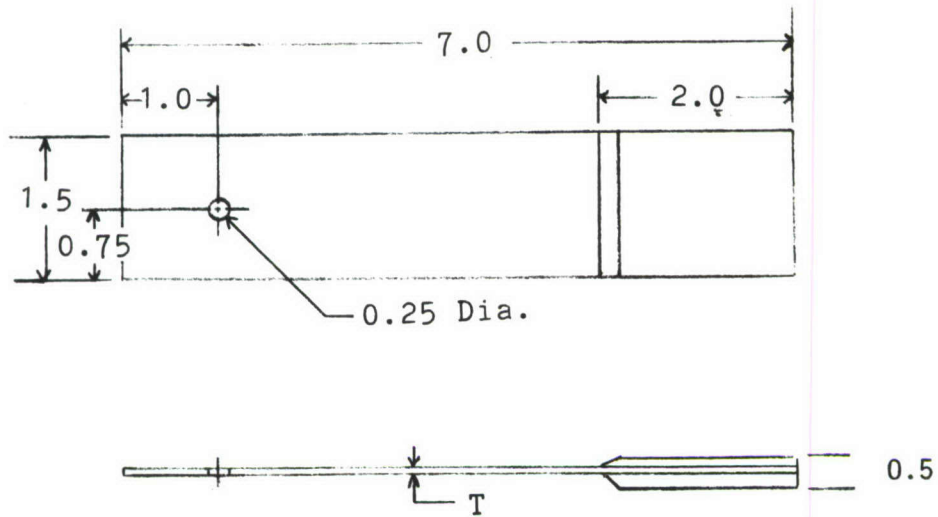


Figure 1 Pin-Bearing Joint Specimen
 (Note: All units are in inches)

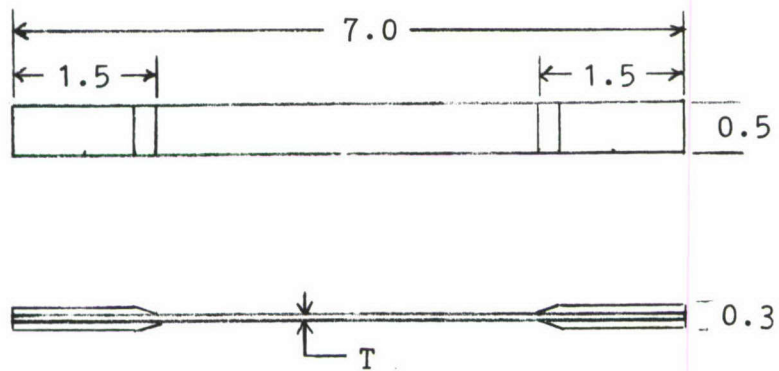


Figure 2 Tensile Test Specimen
 (Note: All units are in inches)

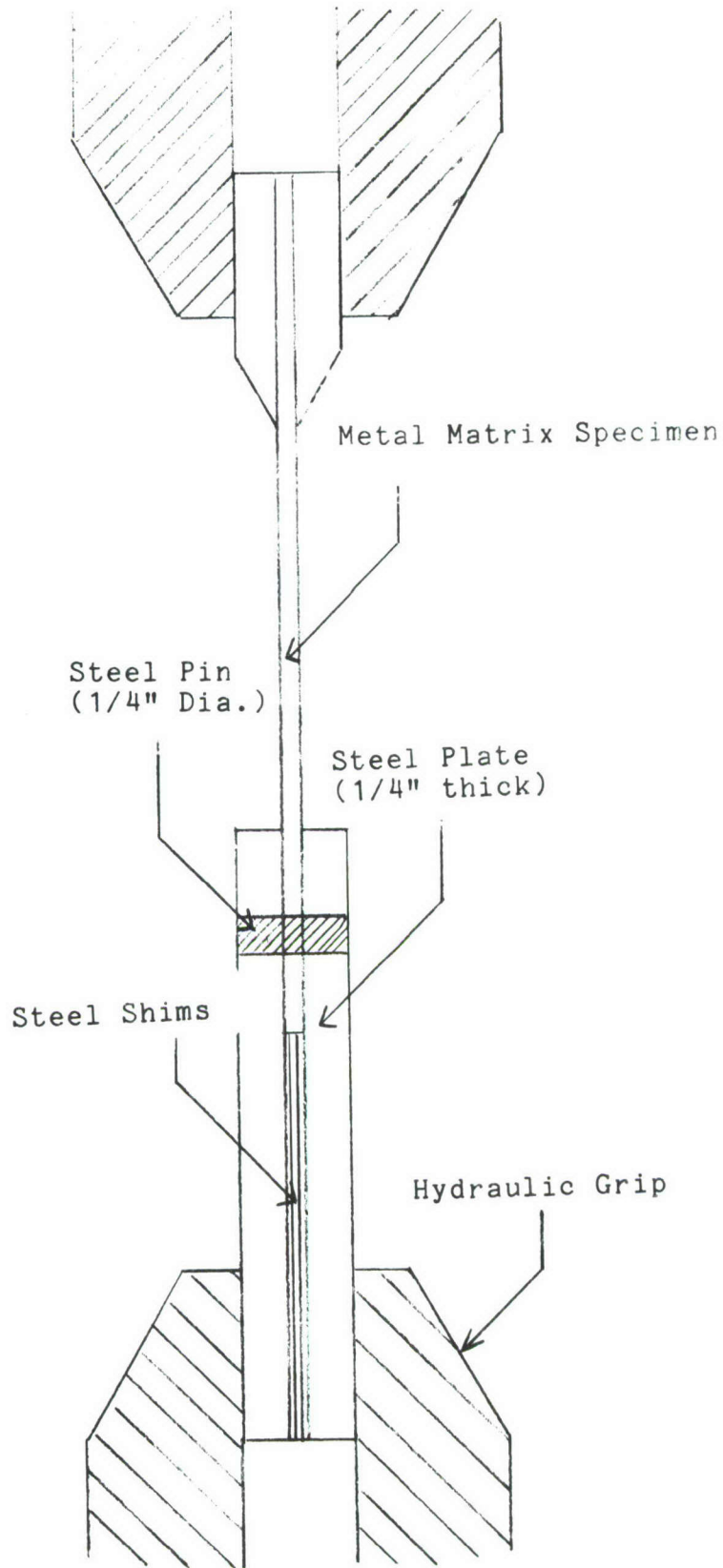


Figure 3 Pin-Bearing Test Assemblage
(Note: Not to scale)

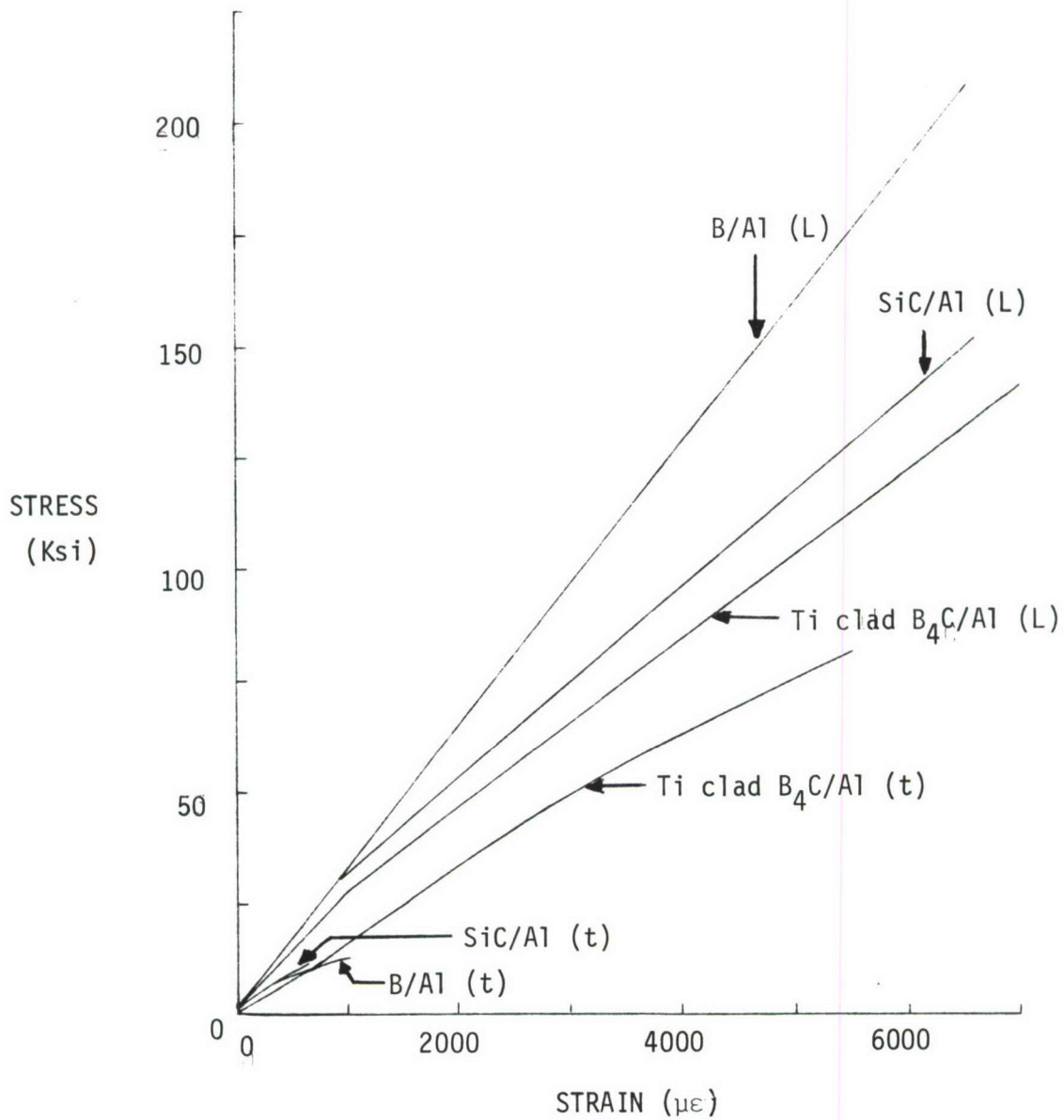


Figure 4 Full Range Stress-Strain Curves

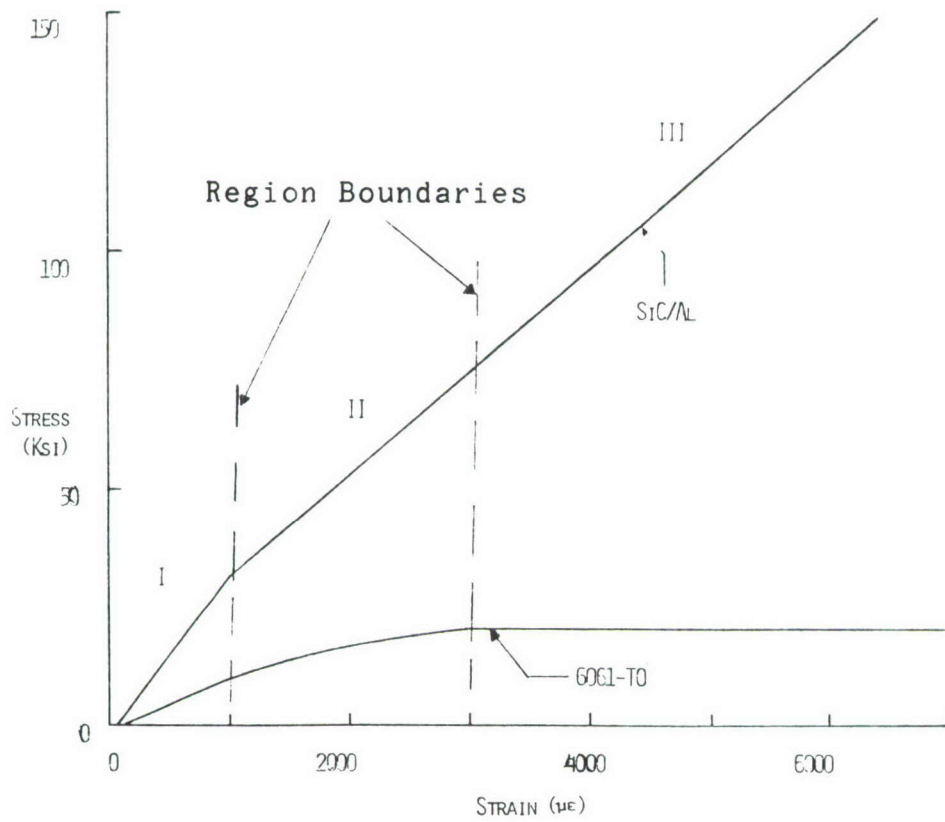


Figure 5 Composite and Matrix Stress-Strain Curves

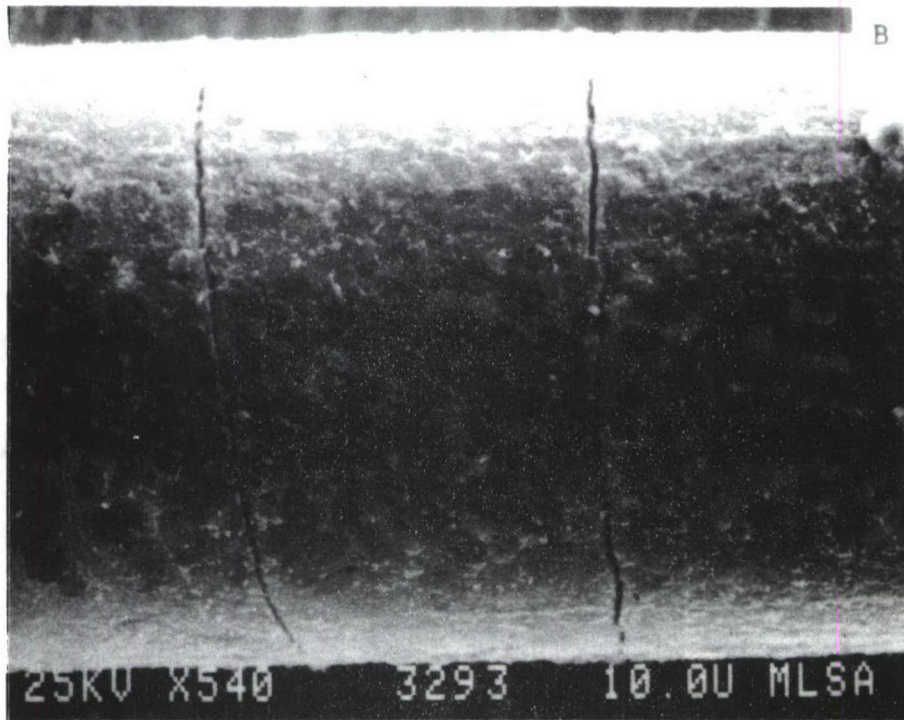
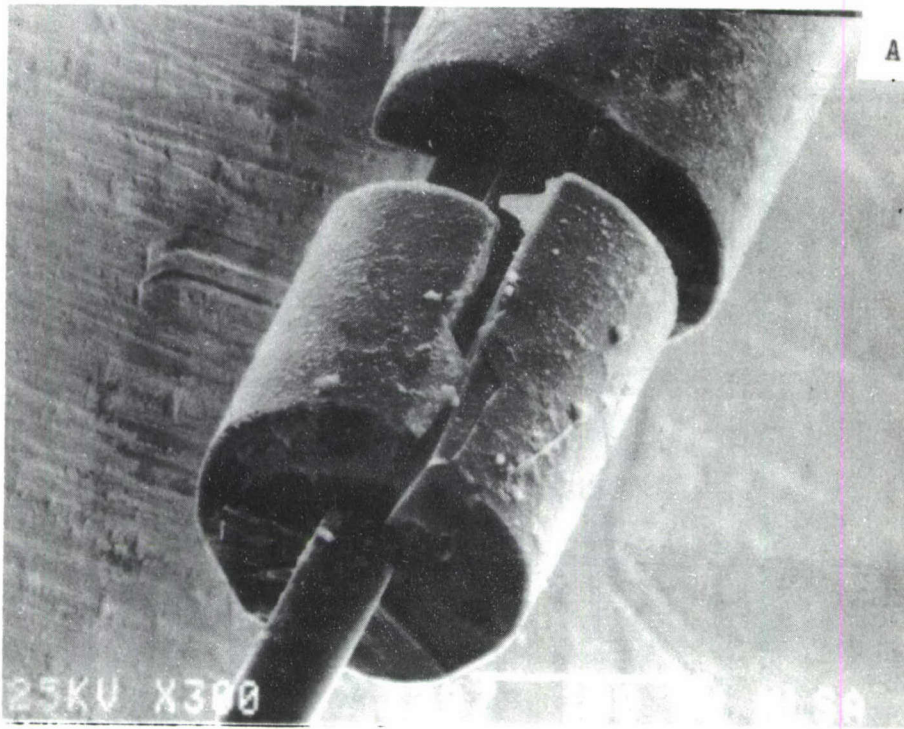


Figure 6 Scanning Electron Microscope Photographs of "limp" Fibers a) 300X b) 540X

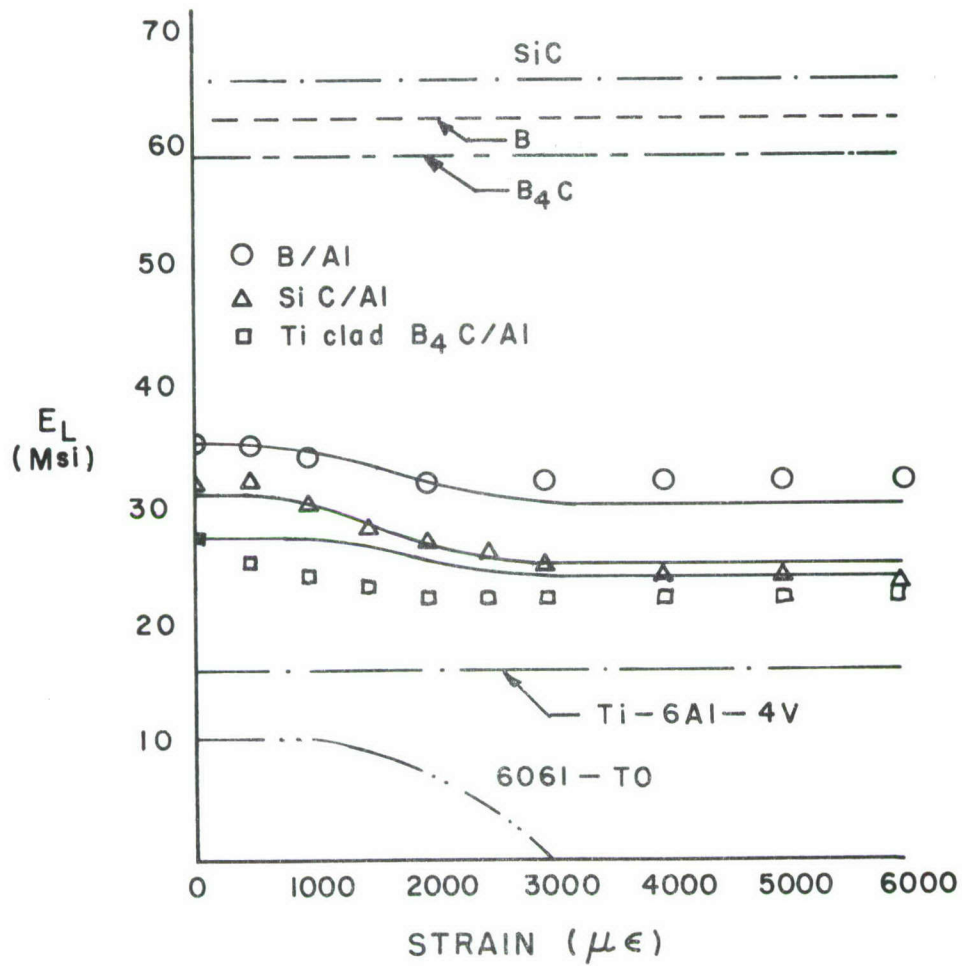


Figure 7 Rule of Mixtures Predictions of Elastic Modulus vs. Strain

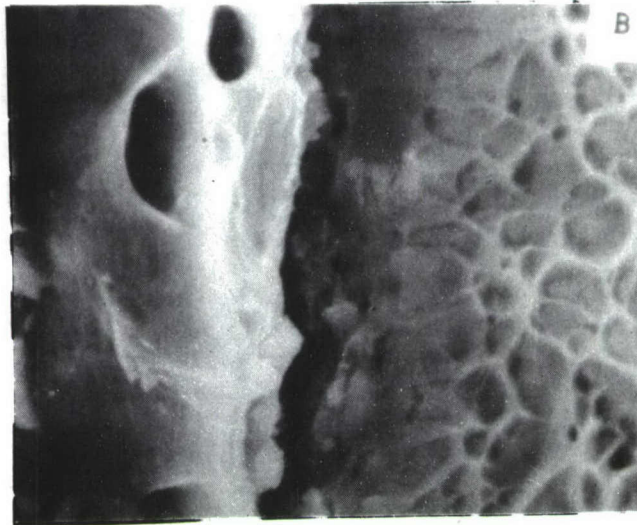
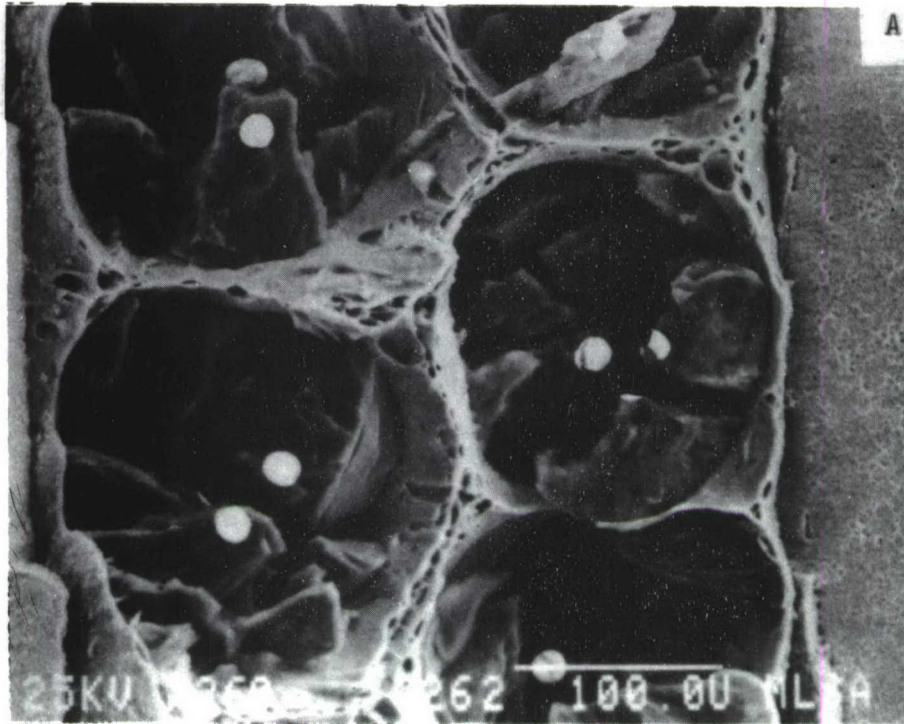


Figure 8 Scanning Electron Microscope Photographs of the Failure Surface of a B_4C/Al Composite clad with Ti-6Al-4V a) Fracture Surface (260X) b) Ti-Al Interface (2000X)

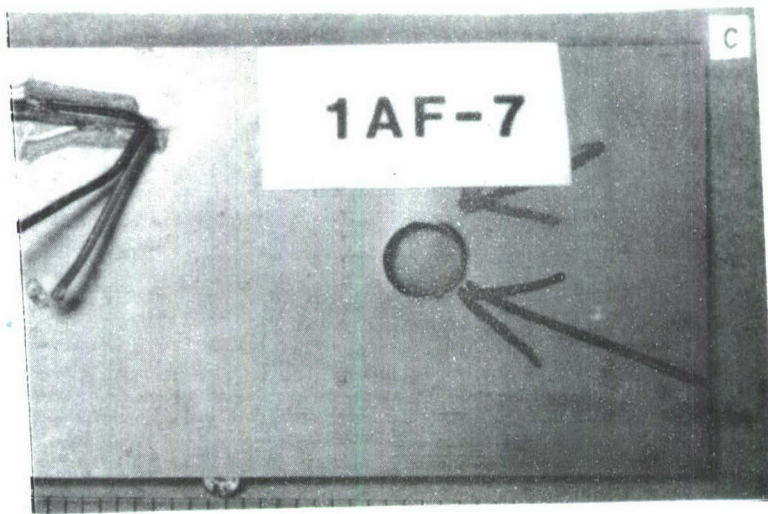
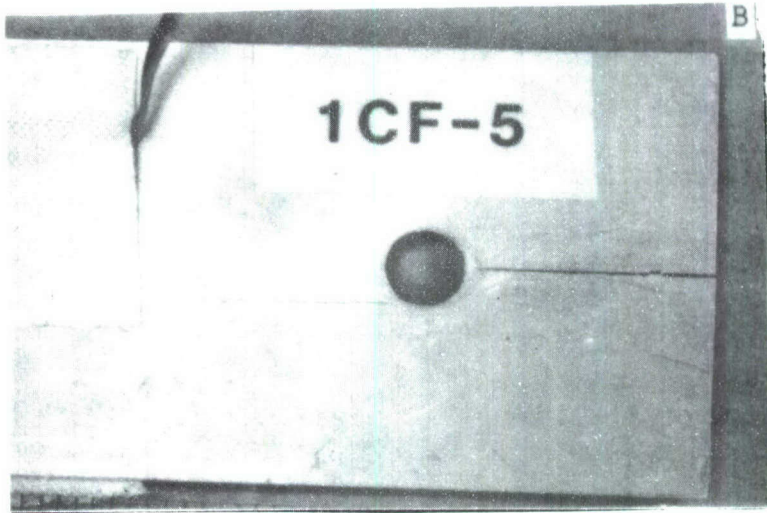
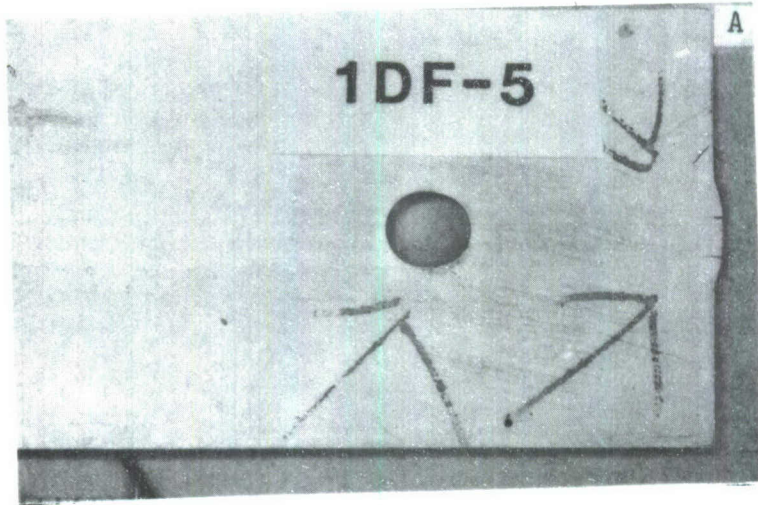


Figure 9 Typical Static Pin-Bearing Joint Failures a) B/Al
b) SiC/Al c) Ti clad B₄C/Al

TABLE 1 Measured Material Property Data

MATERIAL PROPERTY	B/AL		SiC/AL		Ti CLAD B ₄ C/AL	
	L	T	L	T	L	T
NUMBER OF PLIES	8	8	6	6	4*	4*
THICKNESS (IN.)	0.056	0.056	0.051	0.05	0.029	0.029
MODULUS (Msi)	35.0	16.2	31.5	16.3	27.5	15.3
ULT. STRENGTH (Ksi)	201.8	19.0	147.2	11.8	155.1	83.6
POISSON'S RATIO	.31	.15	.28	.17	.29	.16
STRAIN TO FAILURE (MICROSTRAIN)	6196	1734	6833	754	5530	7952

* 2 PLY B₄C/AL, 2 PLY 0.005 IN. Ti-6Al-4V

TABLE 2 Experimental vs. SiC/AL Specimen Dissection Results

	SPECIMEN 1 UNSTRAINED	SPECIMEN 2 REGION II	SPECIMEN 3 REGION III
NUMBER OF FIBER BREAKS	8	19	24
"LIMP" FIBERS	91	86	87
TOTAL FIBERS (LIMP & BROKEN)	99	105	111

TABLE 3 MMC Fiber and Matrix Properties for Rule of Mixtures (R.O.M.) Analysis

MATERIAL	FIBER MODULUS	FIBER VOLUME FRACTION	ALUMINUM MODULUS	ALUMINUM VOLUME FRACTION	Ti MODULUS	Ti VOLUME FRACTION
	E_f	v_f	E_m	v_m	E_{Ti}	v_{Ti}
B/AL	62	.48	10	.52	N/A	N/A
SiC/AL	67	.38	10	.62	N/A	N/A
B ₄ C/AL	58	.32	10	.34	16	.34

TABLE 4 Rule of Mixtures (R.O.M) vs. Literature Fiber Moduli

FIBER	R.O.M.	LITERATURE ²
B _{5.6}	62	56
SiC	67	62
B ₄ C	58	59

Table 5 Measured Ultimate Failure Loads and Modes
the Static Pin-Bearing Specimens

SPECIMEN	B/AL		SiC/AL		Ti Clad B ₄ C/AL	
	P _{fail} (lbs.)	Failure Mode	P _{fail} (lbs.)	Failure Mode	P _{fail} (lbs.)	Failure Mode
1	1225.3	Bearing	998.3	Bearing	714.4	Bearing
2	1473.3	Bearing	979.0	Bearing	790.8	Bearing
3	-	-	1026.6	Bearing	634.5	Bearing
Average	1349.3	Bearing	1001.3	Bearing	713.2	Bearing

Table 6 Average Bearing Stress for the MMC
Pin-bearing Joint Specimens

MATERIAL	BEARING STRESS (Ksi)
B/AL	96.4
SiC/AL	78.5
B ₄ C/AL	98.4

TABLE 7 Mechanical Properties for BJSFM Analysis

MECHANICAL PROPERTY	SiC/AL	B/AL	B ₄ C/AL	TITANIUM
LONGITUDINAL MODULUS	[31.5]	[35.0]	33.4	16
TRANSVERSE MODULUS	[16.3]	[16.2]	20.0	16
SHEAR MODULUS	8.0	9.5	9.5	6.2
POISSON'S RATIO	[0.28]	[0.31]	0.22	0.31
TENSILE LONGITUDINAL ULTIMATE STRENGTH	[147.2]	[201.8]	195.0	134.0
TENSILE TRANSVERSE ULTIMATE STRENGTH	[11.8]	[19.0]	18.7	134.0
COMPRESSION LONGITUDINAL ULTIMATE STRENGTH	280.0	283.0	280.0	134.0
COMPRESSION TRANSVERSE ULTIMATE STRENGTH	20.0	41.0	40.0	134.0
ULTIMATE SHEAR STRENGTH	15.0	22.6	22.0	79.0

NOTE: [] Experimentally Determined; All Other Data for Ref. 2

TABLE 8 BJSFM Predictions vs. Experimental Results

MATERIAL	EXPERIMENTAL	ANALYTICAL	EXP/ANA
B/AL	96.4	91.5	1.05
SIC/AL	78.5	73.0	1.08
B ₄ C/AL	98.4	104.0	0.95

Table 9 Fatigue Test Results

MATERIAL	TEST LOAD (LBS.)	CYCLES TO 0.05 DEFLECTION
B/Al	750	129440
SiC/Al	700	495000
B ₄ C/Al	350	37000

NOTE: All data are the average of 3 specimens